

# Reloc-VGGT: Visual Re-localization with Geometry Grounded Transformer

Tianchen Deng<sup>1\*</sup>, Wenhua Wu<sup>1\*</sup>, Kunzhen Wu<sup>1\*</sup>, Guangming Wang<sup>3</sup>, Siting Zhu<sup>1</sup>,  
Shanghai Yuan<sup>2</sup>, Xun Chen<sup>2</sup>, Guole Shen<sup>1</sup>, Zhe Liu<sup>1</sup>, Hesheng Wang<sup>1</sup>

<sup>1</sup> Shanghai Jiao Tong University <sup>2</sup> Nanyang Technological University <sup>3</sup> Cambridge University

## Abstract

Visual localization has traditionally been formulated as a pair-wise pose regression problem. Existing approaches mainly estimate relative poses between two images and employ a late-fusion strategy to obtain absolute pose estimates. However, late motion average is often insufficient for effectively integrating spatial information, and its accuracy degrades in complex environments. In this paper, we present the first visual localization framework that performs multi-view spatial integration through an early-fusion mechanism, enabling robust operation in both structured and unstructured environments. Our framework is built upon the VGGT backbone, which encodes multi-view 3D geometry, and we introduce a pose tokenizer and projection module to more effectively exploit spatial relationships from multiple database views. Furthermore, we propose a novel sparse mask attention strategy that reduces computational cost by avoiding the quadratic complexity of global attention, thereby enabling real-time performance at scale. Trained on approximately eight million posed image pairs, Reloc-VGGT demonstrates strong accuracy and remarkable generalization ability. Extensive experiments across diverse public datasets consistently validate the effectiveness and efficiency of our approach, delivering high-quality camera pose estimates in real time while maintaining robustness to unseen environments. Our code and models will be publicly released upon acceptance. <https://github.com/dtc11111/Reloc-VGGT>.

## 1. Introduction

Visual re-localization has been a fundamental challenge in robotics and computer vision, which aims to estimate query 6-degree-of-freedom (6-Dof) poses from a database posed images in a world coordinate system. This technology has broad applications in domains including autonomous driving, robotics navigation, VR, and AR, with specific importance in SLAM [21, 25].

\*The first three authors contribute equally to this paper.

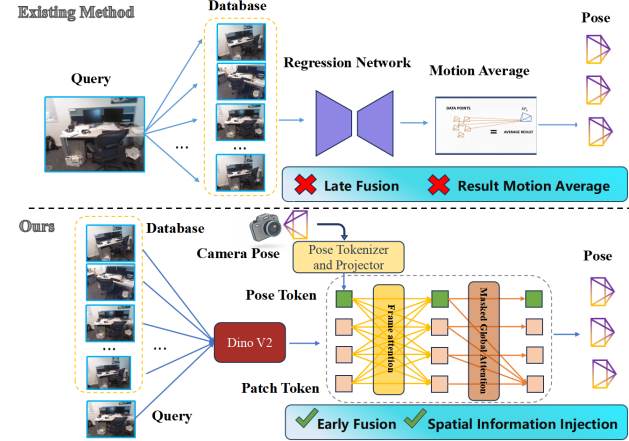


Figure 1. **Illustration of an existing visual relocalization baseline (top) and our proposed method (bottom).** The upper pipeline illustrates conventional relocalization methods, which rely on pair-wise pose regression and employ late fusion to estimate camera poses. In contrast, our approach introduces a multi-frame relocalization framework that performs early fusion through spatial information injection, enabling more effective spatial feature integration. Our method achieves state-of-the-art performance across standard visual relocalization and pose regression benchmarks.

Traditional visual relocalization methods rely on hand-crafted feature points such as ORB [49] or SIFT [52], or on learned features such as SuperPoint [29] and SuperGlue [55], to reconstruct explicit 3D maps. Camera poses are then solved via geometric optimization based on matched 2D–3D correspondences. Alternatively, some recent methods [6–8, 40] avoid explicit map reconstruction and instead recover relative poses directly from neural networks, either by regressing the pose from images or by employing implicit scene representations such as NeRF [46, 72, 76] or 3D Gaussian Splatting [20, 28, 36]. However, these approaches often suffer from limited generalization and typically require ground-truth keypoint correspondences as supervision or per-scene optimization.

Absolute Pose Regression (APR) methods [9, 33, 57, 58, 60, 65] directly estimate the camera pose from images,

providing fast inference and reasonable accuracy, but they remain highly scene-specific and require dense viewpoint coverage during training, which restricts their practical deployment. Relative Pose Regression (RPR) [2, 5, 80] offers a more flexible alternative by predicting the relative pose between a query and a set of database images. These methods avoid per-scene retraining and enable fast execution, but their accuracy remains limited. While several RPR-based methods [2, 30] generalize across datasets, this generalization often comes at the cost of further degraded pose accuracy.

Reloc3R [31] is the first relocalization framework built upon a 3D foundation model. Based on the DUST3R architecture [69], it introduces a motion-averaging strategy to recover absolute poses and achieves strong performance across novel scenes, in both accuracy and test-time efficiency. However, it overlooks multi-frame spatial information by fusing views only through simple motion averaging, which fails to capture geometric relationships under challenging motion or limited viewpoint overlap.

Motivated by this gap, we propose a novel multi-view relocalization framework built on VGGT [68]. First, we introduce a source frame pose tokenizer and projection module to inject spatial relative pose information from multiple reference frames into the network. The injection of pose tokens enables better interaction with the patch and register tokens within the alternating attention block in early fusion, allowing more effective utilization of spatial information, thereby improving pose estimation accuracy. Second, to accelerate test-time inference, we replace the full global attention in VGGT with a sparse mask attention mechanism that retains only the attention between the query and selected anchor frames. This reduces the quadratic attention complexity to linear form ( $\mathcal{O}(N^2) \rightarrow \mathcal{O}(5N - 5)$ ), greatly boosting inference speed and enabling scalable relocalization over long sequences and large environments.

Overall, our contributions are shown as follows:

- We propose a novel multi-frame visual localization method with 3D foundation model, enabling universal generalization across diverse environments, and high camera pose accuracy.
- A novel pose tokenizer and projection module are designed to align the 3D pose token with 2D patch token and better leverage the relative spatial information from multi-view during the attention block.
- We propose a novel sparse mask attention method to further enhance test-time inference speed and reduce memory requirements by reducing the computational complexity from quadratic to linear. Comprehensive experiments across different datasets consistently demonstrate the effectiveness of our proposed framework.

## 2. Related work

Visual relocalization has advanced rapidly and found applications in SLAM [24, 27, 44, 59], navigation [71], autonomous driving [19? ], VR [26]. Here, we review related work on 3D-map based localization, pose regression, and foundation model.

**3D-map based Localization** Traditional 3D-map based methods rely on explicit geometric reconstruction to establish 2D–3D correspondences for pose estimation. Early approaches leverage handcrafted features (e.g., ORB [49], SIFT [52]) or learned local descriptors (e.g., SuperPoint [29], SuperGlue [55]) to match query images with pre-built 3D maps, followed by PnP or bundle adjustment. However, these methods suffer from poor generalization to unseen environments and high computational costs for map construction. Recent implicit scene representations have emerged to avoid explicit map storage. iNeRF [76] pioneered the use of Neural Radiance Fields (NeRF) [46] for camera relocalization, achieving pose optimization by minimizing the photometric error between query images and corresponding renders from a pre-trained NeRF. Lens [48] further enhanced localization accuracy by leveraging NeRF to synthesize additional training data. Building on this line of work, NeRF-SCR [11] introduced uncertainty analysis to improve data efficiency and prevent contamination from low-quality generated samples. More recently, SplatLoc [77] adopted 3D Gaussian Splatting (3DGS) [36] as its scene representation and designed a specialized descriptor decoder for Gaussian primitives, achieving remarkable localization performance. However, these methods require per-scene optimization, which limits their applicability in real-time scenarios.

**Pose Regression** Pose regression methods directly estimate camera poses from images without explicit 3D maps, divided into Absolute Pose Regression (APR) and Relative Pose Regression (RPR). APR methods directly regress 6-DoF camera poses from query images. PoseNet [35] pioneers the use of convolutional neural networks to predict camera poses directly from individual images. Subsequently, VidLoc [16] extends to sequential images, leveraging temporal continuity to achieve enhanced pose estimation accuracy and smoothness. Further advancing this direction, LSG [74] incorporates relative pose constraints from visual odometry to refine camera tracking. However, these methods exhibit inherent limitation in scene generalization, typically requiring retraining for new scenes. RPR methods predict relative poses between query and reference images, offering enhanced flexibility. RelocNet [5] introduces feature descriptors learned through nearest-neighbor matching and continuous metric learning to achieve relative pose regression between query images and their nearest neighbors. CamNet [30] proposes a coarse-to-fine learning framework that progressively refines

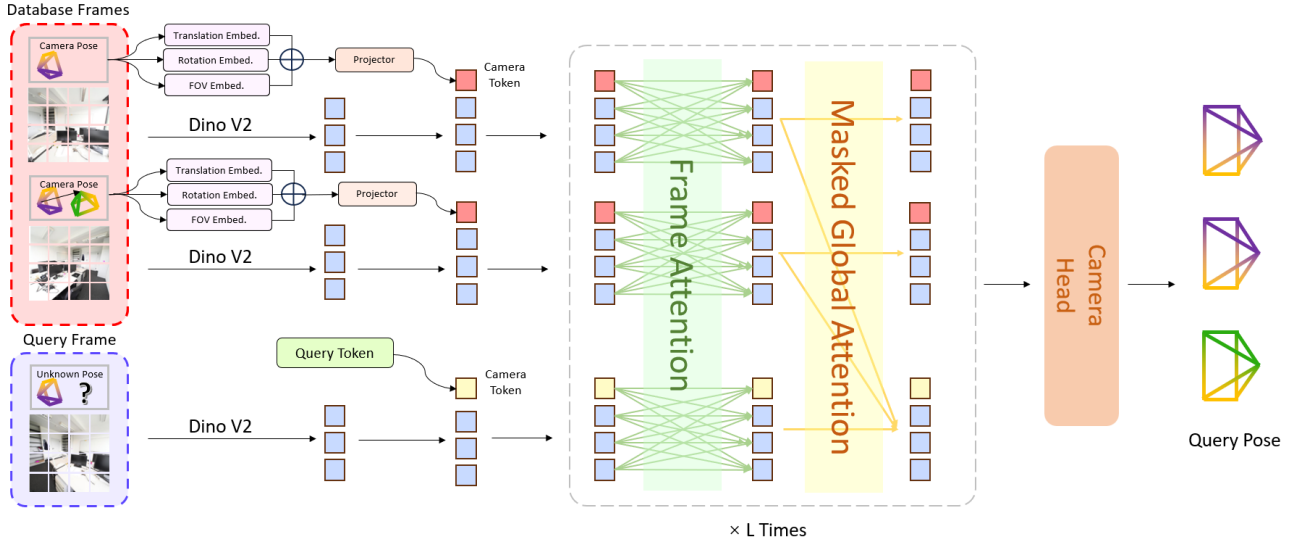


Figure 2. **System Overview.** We propose a novel visual re-localization framework with 3D foundation model. We introduce a novel pose tokenizer and projection module to better leverage the spatial information for early fusion and design a sparse mask attention strategy to enhance test-time inference speed and reduce computational complexity from quadratic to linear.

pose estimation accuracy. Relpose-GNN [63] constructs graph structures connecting query and reference images, enabling efficient feature propagation to obtain consistent camera poses. Despite demonstrating better generalization capabilities than APR methods, these RPR approaches still require dataset-specific training and thus remain limited in scalability.

**Foundation Model** The Transformer architecture [64] has been widely adopted in large-scale vision models [4, 37, 51] and language models [3, 15, 47]. With the advancement of large-scale pretrained models, 3D vision foundation models [23] have attracted significant research attention. DUST3R [69] introduces a novel paradigm for 3D reconstruction from image collections without requiring camera poses or calibration parameters, unifying various 3D vision tasks under a single framework. MUST3R [10] extends the pairwise formulation to multi-view scenarios and incorporates a multi-layer memory mechanism, substantially improving reconstruction efficiency. VGGT [68] presents an elegantly designed feed-forward network that directly infers all essential 3D attributes from image collections with remarkable efficiency. Notably, Reloc3R [31] pioneers the application of such models to visual relocalization tasks. However, its multi-view fusion relies solely on simple averaging strategies, failing to fully exploit inter-frame geometric relationships. In contrast, our method leverages relative pose token injection and sparse attention mechanisms to comprehensively capture geometric correlations between frames and maintain real-time performance.

### 3. Method

We propose Reloc-VGGT, a universal visual re-localization framework. The input to our method consists of query and source images  $\{\mathbf{I}_i\}$  from database and the relative 6DOF camera poses  $\{R_i, T_i\}$  of source images. The output of our framework is the estimated poses to the world coordinate system defined by the database images. Fig. 2 illustrates an overview of the proposed framework. It is composed of two main modules: (i) relative pose regression (ii) pose tokenizer and projector (Sec. 3.2); (iii) sparse mask attention (Sec. 3.3); We elaborate on the entire pipeline of our system in the following subsections.

#### 3.1. Relative Pose Regression

For each query image  $I_q$ , we retrieve the top- $K$  nearest database images using an off-the-shelf image retrieval method [1], forming a set of source–query pairs  $\mathbf{Q} = (I_{d_k}, I_q) | k = 1, \dots, K$ . The pose of the query image is then estimated based on the known poses of these source images. Existing methods, such as Reloc3R [31], typically perform pairwise matching between the query and each source image and then fuse the results by averaging the predicted motions. In contrast, our approach performs multi-frame matching, enabling more effective aggregation of spatial information through alternating frame attention and global attention.

We adopt VGGT [68] as the 3D backbone of our relative pose regression network. Given the query image, the  $K$  retrieved source images, and their corresponding known poses, the network directly predicts the pose of the query

image. Formally, the process can be expressed as:

$$\{R, T\}_q = f_\theta(I_q, \{(I_{d_k}, \{R, T\}_{d_k})\}_{k=1}^K), \quad (1)$$

where  $\{R, T\}_{d_k}$  denotes the known pose of the  $k$ -th source image, and  $\{R, T\}_q$  is the predicted pose of the query image. For the camera parameters  $\{R, T\}$ , we follow the parametrization from [68], where the rotation matrix is represented using a quaternion, and an additional field-of-view (FoV) term is included. These components are then concatenated into a single vector, consisting of the rotation quaternion  $\mathbf{q} \in \mathbb{R}^4$ , the translation vector  $\mathbf{t} \in \mathbb{R}^3$ , and the field-of-view parameter  $\mathbf{f} \in \mathbb{R}^2$ . We assume that the camera's principal point is at the image center, which is common in SfM frameworks [56].

For the query frame within the input sequence, we explore two different placement strategies. The first is to treat the query frame as the anchor frame, leveraging VGGT's design where the first frame is interpreted as the world coordinate system. In this case, the final absolute pose can be obtained directly by motion averaging. However, this approach makes it impossible to inject relative pose tokens, since the pose of the query frame is unknown at inference time. Alternatively, since VGGT treats all non-anchor frames symmetrically, we position the query frame at the last index of the sequence and select the most similar database frame—identified using visual place recognition methods [1, 22]—as the anchor frame. This setup allows us to encode and inject relative pose tokens for all other source frames, including those associated with the query.

### 3.2. Pose Tokenizer and Projector

Unlike previous pose regression methods that rely on late fusion to combine source image poses, we adopt an intermediate fusion strategy. Specifically, we encode the relative pose between the query and source images and align it with the register and patch tokens before feeding them into the alternating attention blocks. This design enables more effective spatial reasoning and feature interaction across multiple frames.

Building upon this, we apply learnable Fourier embeddings [46] to encode the relative translation vector, the rotation quaternion, and the field-of-view (FoV) parameters:

$$\begin{aligned} \gamma(\mathbf{t}) &= [\sin(2^l \pi \mathbf{t}), \cos(2^l \pi \mathbf{t})]_{l=0}^{L_t-1}, \\ \gamma(\mathbf{q}) &= [\sin(2^l \pi \mathbf{q}), \cos(2^l \pi \mathbf{q})]_{l=0}^{L_d-1}, \\ \gamma(\mathbf{f}) &= [\sin(2^l \pi \mathbf{f}), \cos(2^l \pi \mathbf{f})]_{l=0}^{L_f-1}. \end{aligned} \quad (2)$$

We set  $L_t = 10, L_d = 4, L_f = 4$ . Finally, we introduce a camera token projector, implemented as an MLP, to align the register tokens, 2D patch tokens with the 3D camera tokens, thereby enhancing the spatial consistency of

sequence-level representations.

$$\mathbf{f}_{cam} = \text{MLP}_{cam}(\gamma(\mathbf{x}), \gamma(\mathbf{q}), \gamma(\mathbf{f})) \quad (3)$$

### 3.3. Sparse Mask Attention

In the original VGGT architecture, the alternating attention framework consists of two types of blocks: frame attention and global attention. While this design achieves highly accurate pose estimation, the global attention module introduces significant computational overhead with a quadratic complexity of  $\mathcal{O}(n^2)$ —particularly problematic when the sequence length increases. Recent works such as FastVGGT [61] have analyzed attention maps and revealed substantial redundancy in global attention, uncovering a key insight: attention patterns across tokens exhibit a high degree of similarity, resulting in large portions of unnecessary computation, a phenomenon also observed in models like DINOv2 [50].

Motivated by these observations, we propose a task-specific sparse mask attention mechanism tailored for visual re-localization. As illustrated in Fig. 3, we compare the original global attention in VGGT, the masked attention in StreamVGGT [81], and our proposed sparse mask attention. Our method significantly reduces redundant attention computation while maintaining accuracy, making it feasible to perform multi-frame relocalization efficiently at large scales.

**Design Rationale.** In the VGGT architecture, the first frame is defined as the world coordinate system, with all tokens registered relative to this reference frame. This setup, along with the subsequent training pipeline, makes the first frame a crucial anchor for maintaining spatial consistency throughout the sequence. Therefore, we preserve all attention connections associated with the anchor frame. Second, as shown in the second illustration of Fig. 3, StreamVGGT adopts a causal mask because its sequential streaming input allows each frame to attend only to previous frames. However, our task only requires estimating the pose of the query frame, so we retain all attention interactions involving the query frame as well. This corresponds to the structure shown in Fig. 3.

Beyond these interactions, we further find a dilated attention mask for the remaining source frames to sparsify computation while still preserving the necessary spatial context. Nevertheless, this approach still incurs substantial computation and relatively slow inference, and its performance is inferior to the proposed sparse mask attention mechanism.

To this end, we propose the proposed sparse mask attention strategy and introduce it into the global attention block. It reduces the quadratic attention complexity to linear form ( $\mathcal{O}(N^2) \rightarrow \mathcal{O}(5N - 5)$ ), transforming global attention into a scalable component suitable for long-sequence relocalization.

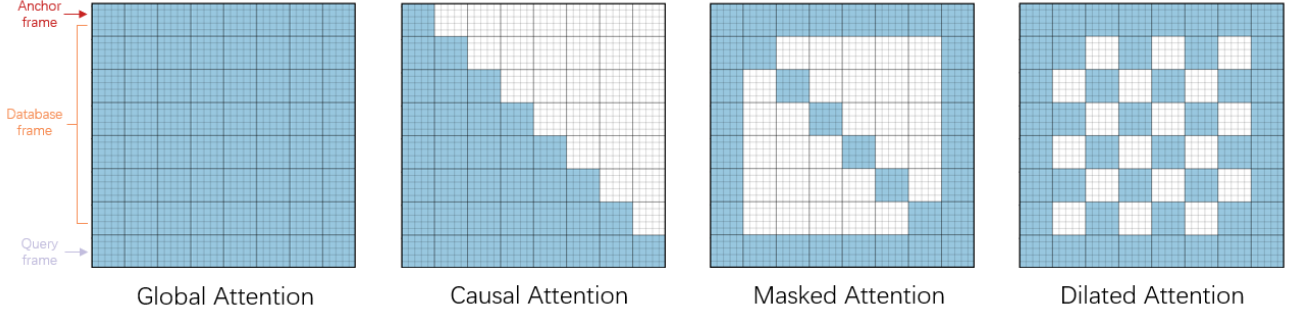


Figure 3. We visualize the global attention maps under different masking strategies. From left to right, the figures correspond to the original global attention in VGGT, the causal attention in StreamVGGT [81], and our proposed sparse mask attention and dilated mask attention.

### 3.4. Training Loss

The output of our network consists of three components: 1) the rotation quaternion, which captures the relative change in camera orientation, 2) the translation vector, which represents the change in camera position, and 3) the field-of-view (FoV), which encodes the camera’s intrinsic parameters. To supervise these outputs, we adopt an  $\mathcal{L}_1$  loss function. Since translation is sensitive to scene scale, we apply a scale-aware transformation to the translation vector in the loss:

$$\mathcal{L}_{\text{pose}} = \sum_{i=0}^K \left( \|\hat{\mathbf{q}}_i - \mathbf{q}_i\| + \|\hat{\mathbf{t}}_i - \mathbf{t}_i\| + \|\hat{\mathbf{f}}_i - \mathbf{f}_i\| \right) \quad (4)$$

Jointly supervising all three components stabilizes training and allows the model to converge more rapidly. We also use the rotation loss from [31] to enhance the learning of rotation components  $\mathcal{L}_R = \arccos\left(\frac{\text{tr}(\hat{R}^{-1}R) - 1}{2}\right)$ . Our training process follows a two-stage strategy. In the first stage, we freeze the ViT encoder and decoder, and only train the pose tokenizer and projector. This ensures that the injected pose tokens are properly aligned with the original register and patch tokens. In the second stage, we unfreeze the decoder and attention blocks and proceed with end-to-end training.

## 4. Experiments

In this section, we first describe the implementation details, training datasets, and baseline methods used for comparison. We then present results across various test datasets, covering both two-frame pairwise relative pose estimation and full visual relocalization experiments. Finally, we conduct ablation studies and additional analyses to evaluate the effectiveness of each component in our framework.

### 4.1. Implementation Details

Our model architecture follows VGGT [68] with  $L = 24$  alternating frame and global attention layers. To accelerate inference, we incorporate FlashAttention-2 [18]. The model is initialized using pre-trained VGGT weights. We train using the AdamW optimizer with a hybrid learning rate schedule: a linear warm-up over the first 0.5 epochs, followed by cosine decay, with a peak learning rate of  $1 \times 10^{-6}$ . All experiments are conducted on 4 NVIDIA A100 GPUs.

For the visual localization task, following Reloc3R [31], we adopt NetVLAD [1] for image retrieval and select the top 10 most similar image pairs without applying distance-based clustering.

### 4.2. Dataset and Baseline

The choice of training datasets follows Reloc3R [31]. Each input image is center-cropped based on its principal point and resized to a fixed width of 518 pixels. For the pairwise relative camera pose estimation experiments, we evaluate on the ScanNet1500 [17] datasets. Following previous research [31], we employ three metrics in pair-wise experiments: AUC@5/10/20. These metrics calculate the area under the curve of pose accuracy using thresholds of  $\tau = 5/10/20$  degrees for the minimum of rotation and translation angular errors. For multi view relative pose experiments, we conduct the evaluation on the CO3Dv2 [53] dataset. We use the metrics in [66, 69] RRA@15 the relative rotation accuracy within 15 degrees, and RTA@15 for the relative translation accuracy within 15 degrees. the mean average accuracy (mA@30, also called AUC@30). To evaluate the visual re-localization experiments, we conduct evaluations on two public benchmarks that cover both indoor and outdoor environments: the 7-Scenes dataset [62] and the Cambridge Landmarks dataset [34]. for each scene, we report the median translation and rotation errors (in meters and degrees, respectively).

Methods	ScanNet1500			Inference time
	AUC@5	AUC@10	AUC@20	
Non-PR	Efficient LoFTR [70]	19.20	37.00	53.60
	ROMA [32]	28.90	50.40	68.30
	DUS3R [69]	23.81	45.91	65.57
	MAS3R [10]	28.01	50.24	68.83
	NoPoSplat [75]	31.80	53.80	>2000 ms
PR	Map-free (Regress-SN) [2]	1.84	8.75	25.33
	Map-free (Regress-MF) [2]	0.50	3.48	13.15
	ExReNet (SN) [73]	2.30	10.71	26.13
	ExReNet (SUNCG) [73]	1.61	7.00	18.03
	Reloc3r-512 [31]	34.79	58.37	75.56
	<b>Reloc-VGGT</b>	<b>36.35</b>	<b>58.62</b>	<b>75.90</b>
				45 ms

Table 1. Pair-wise relative pose estimation experiments on the ScanNet1500 dataset [17].

	Methods	RRA@15	RTA@15	mAA@30
Non-PR	PixSfM [43]	33.7	32.9	30.1
	RelPose [78]	57.1	-	-
	PoseDiffusion [66]	80.5	79.8	66.5
	RelPose++ [41]	82.3	77.2	65.1
	RayDiffusion* [79]	93.3	-	-
	VGGSFm [67]	92.1	88.3	74.0
	DUS3R (w/ PnP) [69]	94.3	88.4	77.2
	MAS3R [39]	94.6	91.9	81.1
PR	PoseReg [66]	53.2	49.1	45.0
	RayReg* [79]	89.2	-	-
	Reloc3r-512 [31]	95.8	93.7	82.9
	<b>Reloc-VGGT</b>	<b>96.1</b>	<b>94.5</b>	<b>83.4</b>

Table 2. Multi-frame relative pose evaluation the CO3Dv2 dataset [53].

### 4.3. Relative Camera Pose Estimation

**Pair-wise relative pose** In this section, we evaluate the accuracy of pair-wise relative pose estimation. The results are shown in Tab. 1. We compare our method with several state-of-the-art approaches, including Dust3R [69], NopoSplat [75], Map-Free [2], and ExReNet [73]. Experimental results demonstrate that our method achieves competitive performance in two-view matching and pose estimation tasks.

**Multi-view relative pose** The multi-view pose estimation results are shown in Tab. 2. We compare Reloc3r with recent SfM-based approaches, PixSfM [43] and VGG-SfM [67], as well as data-driven methods including RelPose [78], RelPose++ [41], PoseDiffusion [66], RayDiffusion [79], DUS3R (with PnP) [69], and MAS3R [39]. Unlike Reloc3r, which aggregates pairwise predictions, our method more effectively integrates information across multiple frames, enabling consistent multi-view matching and robust joint pose estimation. This richer temporal and cross-view fusion leads to improved geometric consistency and strengthens pose recovery in challenging multi-view scenarios.

ios.

### 4.4. Visual Re-localization

In this section, we evaluate the absolute pose estimation capability of our approach. Tab. 3 reports results on the indoor 7-Scenes dataset [62]. We compare our method against state-of-the-art absolute pose regression (APR) and relative pose regression (RPR) approaches. Following the evaluation protocol of Reloc3R, we additionally distinguish between seen and unseen scenes, where the latter contains entirely novel environments during testing. Across both settings, our method consistently achieves state-of-the-art performance in terms of translation and rotation errors. In unseen scenes, the performance gap becomes even more pronounced, demonstrating the strong generalization ability of our design. These results clearly validate the effectiveness of our early fusion module, which integrates relative pose cues from the input sequence to produce more accurate and stable absolute pose estimates. Moreover, compared with APR methods, our approach attains superior accuracy without any scene-specific training, highlighting its robustness and adaptability across diverse environments.

Tab. 4 further presents results on the outdoor Cambridge Landmarks dataset [45], a widely used benchmark for regression-based localization. In this more challenging outdoor setting, all RPR methods—under both seen and unseen configurations—experience notable performance degradation. Nevertheless, our method still achieves a significant improvement over existing approaches, including the foundation-model-based Reloc3R, yielding substantially lower translation and rotation errors. This confirms the strength of our overall architecture, where the pose tokenizer, pose projector, and the associated early fusion and spatial information injection collectively contribute to robust global pose estimation. Although the introduction of sparse mask attention brings a slight reduction in accuracy, it achieves a favorable balance between accuracy and computational efficiency, making the model more suitable for real-world deployment. Visual comparisons are provided in Fig. 4.

### 4.5. Ablation Studies

To validate the effectiveness of each core component in Reloc-VGGT, we conducted systematic ablation experiments on the 7-Scenes and Cambridge Landmarks datasets. All experiments maintained identical configurations to ensure fair comparisons.

First, we verified the necessity of the two proposed core modules: the relative Pose Tokenizer and Projection (RPTP) and Sparse Mask Attention (SMA). The experimental configurations were designed as follows: a. Retain the backbone network but remove the aforementioned two modules, and SMA with full global attention, the same with

Methods	Chess	Fire	Heads	Office	Pumpkin	RedKitchen	Stairs	Average	Dataset-specific training time
<b>APR</b>									
LENS [48]	0.03 / 1.30	0.10 / 3.70	0.07 / 5.80	0.07 / 1.90	0.08 / 2.20	0.09 / 2.20	0.14 / 3.60	0.08 / 3.00	Days / scene
PMNet [42]	0.03 / 1.26	0.04 / 1.76	0.06 / 1.68	0.06 / 1.90	0.07 / 1.91	0.08 / 2.23	0.11 / 2.97	0.06 / 1.96	Days / scene
DFNet [12]+NeFeS [13]	<b>0.02 / 0.57</b>	<b>0.02 / 0.74</b>	<b>0.02 / 1.28</b>	<b>0.02 / 0.56</b>	<b>0.02 / 0.55</b>	<b>0.02 / 0.57</b>	<b>0.05 / 1.28</b>	<b>0.02 / 0.79</b>	Days / scene
Marepo [14]	0.02 / 1.24	<b>0.02 / 1.39</b>	<b>0.02 / 2.03</b>	0.03 / 1.26	0.04 / 1.48	0.04 / 1.71	0.06 / 1.67	0.03 / 1.54	15min / scene
<b>RPR (Seen)</b>									
EssNet (7S) [80]	–	–	–	–	–	–	–	0.22 / 8.03	Hours
Relative PN (7S) [38]	0.13 / 6.46	0.26 / 12.72	0.14 / 12.34	0.21 / 7.35	0.24 / 6.35	0.24 / 8.03	0.27 / 11.82	0.21 / 9.30	Hours
NC-EssNet (7S) [80]	0.26 / 10.44	–	0.26 / 10.4	0.18 / 5.32	–	0.23 / 7.45	–	0.21 / 7.50	Hours
RelocNet (7S) [5]	0.12 / 4.14	0.21 / 7.50	0.13 / 8.70	0.15 / 4.50	0.13 / 5.30	0.21 / 5.08	0.28 / 7.53	0.16 / 5.73	Hours
Relpose-GNN [7]	0.08 / 2.70	0.21 / 5.30	0.13 / 8.70	0.15 / 4.30	0.13 / 5.09	0.19 / 5.30	0.22 / 6.50	0.16 / 5.20	Hours
AnchorNet [54]	0.06 / 3.89	0.15 / 10.3	0.08 / 10.9	0.09 / 4.90	0.20 / 2.97	0.08 / 4.68	0.10 / 9.26	0.09 / 6.74	Hours
CamNet [30]	<b>0.04 / 1.73</b>	<b>0.03 / 1.74</b>	<b>0.05 / 1.98</b>	<b>0.04 / 1.62</b>	<b>0.04 / 1.64</b>	<b>0.04 / 1.63</b>	<b>0.04 / 1.51</b>	<b>0.04 / 1.69</b>	Hours
<b>RPR (Unseen)</b>									
EssNet (CL) [80]	–	–	–	–	–	–	–	0.57 / 80.06	None
NC-EssNet (CL) [80]	–	–	–	–	–	–	–	0.48 / 32.97	None
Relative PN (U) [38]	0.31 / 15.05	0.40 / 19.00	0.24 / 22.15	0.38 / 14.14	0.44 / 18.24	0.41 / 16.51	0.35 / 23.55	0.36 / 18.38	None
RelocNet (SN) [5]	0.21 / 10.9	0.28 / 11.4	0.23 / 11.8	0.31 / 10.3	0.40 / 10.9	0.33 / 11.4	0.33 / 11.4	0.29 / 11.3	None
ImageNet+NCM [80]	–	–	–	–	–	–	–	0.19 / 4.30	None
Map-free (Match) [2]	0.10 / 2.93	0.12 / 4.95	0.11 / 5.44	0.12 / 3.77	0.14 / 3.45	0.14 / 4.45	0.14 / 4.50	0.12 / 4.07	None
Map-free (Regress) [2]	0.09 / 2.64	0.13 / 4.54	0.11 / 4.81	0.11 / 3.77	0.13 / 3.11	0.13 / 4.11	0.13 / 4.70	0.12 / 3.95	None
ExReNet (SN) [73]	0.06 / 3.30	0.09 / 5.20	0.09 / 3.04	0.07 / 2.17	0.11 / 2.75	0.09 / 3.47	0.09 / 7.74	0.09 / 3.95	None
ExReNet (SUNCG) [73]	0.05 / 2.75	0.07 / 2.60	0.08 / 3.00	0.07 / 2.17	0.09 / 2.75	0.07 / 3.47	0.07 / 7.74	0.07 / 3.07	None
Reloc3r-512 [31]	0.027 / 0.882	0.028 / <b>0.805</b>	<b>0.013 / 0.953</b>	0.041 / 0.876	0.062 / 1.105	0.043 / 1.264	0.070 / 1.357	0.041 / 1.035	None
Reloc-VGGT (mask)	0.027 / 0.861	0.028 / 0.871	0.014 / 0.818	0.039 / 0.850	0.053 / 1.213	0.042 / 1.480	0.074 / 1.178	0.039 / 1.033	None
Reloc-VGGT	<b>0.025 / 0.767</b>	<b>0.024 / 0.833</b>	<b>0.013 / 0.770</b>	<b>0.036 / 0.827</b>	<b>0.048 / 1.040</b>	<b>0.039 / 1.249</b>	<b>0.038 / 0.776</b>	<b>0.031 / 0.896</b>	None

Table 3. Pose estimation results (median translation / rotation error) on the 7-Scenes dataset [62]. APR: absolute pose regression; RPR: relative pose regression.

Methods	GreatCourt	KingsCollege	OldHospital	ShopFacade	StMarysChurch	Average (4)	Average	Dataset-specific training time
<b>APR</b>								
LENS [48]	–	0.33 / <b>0.50</b>	0.44 / 0.90	0.27 / 1.60	0.53 / 1.60	0.39 / 1.20	–	Days / scene
PMNet [42]	–	0.31 / 0.55	0.44 / 0.79	0.17 / 0.86	0.31 / 0.96	0.31 / 0.79	–	Days / scene
DFNet [12]+NeFeS [13]	–	0.37 / 0.54	0.52 / 0.88	<b>0.15 / 0.53</b>	0.37 / 1.14	<b>0.35 / 0.77</b>	–	Days / scene
<b>RPR (Seen)</b>								
EssNet (CL) [80]	3.20 / 2.20	0.48 / 1.00	1.14 / 2.50	0.48 / 2.50	1.52 / 3.20	1.08 / 3.41	1.37 / 2.30	Hours
Relpose-GNN [7]	–	–	–	–	–	0.91 / 2.30	0.85 / 2.82	Hours
NC-EssNet [80] (CL)	–	–	–	–	–	–	–	Hours
AnchorNet [54]	–	0.57 / 0.88	1.21 / 2.55	0.52 / 2.27	1.04 / 2.69	0.84 / 2.10	–	Hours
<b>RPR (Unseen)</b>								
EssNet (7S) [80]	–	–	–	–	–	10.36 / 85.75	–	None
NC-EssNet (7S) [80]	–	–	–	–	–	9.78 / 24.35	–	None
Map-free (Match) [2] †	9.09 / 5.33	2.51 / 3.11	3.89 / 6.44	1.04 / 3.61	3.00 / 6.14	2.61 / 4.83	3.90 / 4.93	None
Map-free (Regress) [2]	8.40 / 4.56	2.44 / 2.54	3.73 / 5.23	0.97 / 3.17	2.91 / 5.10	2.51 / 4.01	3.69 / 4.12	None
ExReNet (SN) [73]	10.97 / 6.52	2.34 / 2.99	3.40 / 4.92	0.90 / 3.23	2.60 / 4.69	2.36 / 4.23	4.08 / 4.32	None
ExReNet (SUNCG) [73]	9.79 / 4.46	2.33 / 2.48	3.54 / 3.49	0.72 / 2.41	2.30 / 3.74	2.22 / 3.03	3.74 / 3.31	None
ImageNet+NCM [80] †	–	–	–	–	–	1.83 / 0.56	–	None
Reloc3r-512 [31]	1.22 / 0.73	0.42 / 0.36	0.62 / 0.55	0.13 / 0.58	0.34 / 0.58	0.38 / 0.52	0.55 / 0.56	None
Reloc-VGGT(mask)	0.98 / 0.63	0.40 / 0.48	0.59 / 0.52	0.14 / 0.56	0.31 / 0.55	0.36 / 0.55	0.48 / 0.55	None
Reloc-VGGT	<b>0.59 / 0.43</b>	<b>0.36 / 0.36</b>	<b>0.57 / 0.44</b>	<b>0.10 / 0.33</b>	<b>0.24 / 0.43</b>	<b>0.32 / 0.37</b>	<b>0.37 / 0.38</b>	None

Table 4. Pose estimation results (median translation / rotation error) on the Cambridge Landmarks [34] dataset. APR: absolute pose regression; RPR: relative pose regression.

VGVT. b. Remove only the relative Pose Tokenizer and Projection (RPTP). c. Remove only the Sparse Mask Attention (SMA).

The experimental results are presented in Tab. 5. It can be observed that after incorporating RPTP, the average translation/rotation errors are significantly reduced. This demonstrates that relative pose regression enables effective

interaction between spatial information and visual features, thereby enhancing the accuracy of pose estimation. When SMA is used alone, the inference time is reduced by 35% compared to the baseline model, with only minor performance degradation. This validates that sparse attention with linear complexity can efficiently reduce redundant computations without losing critical geometric context. The full

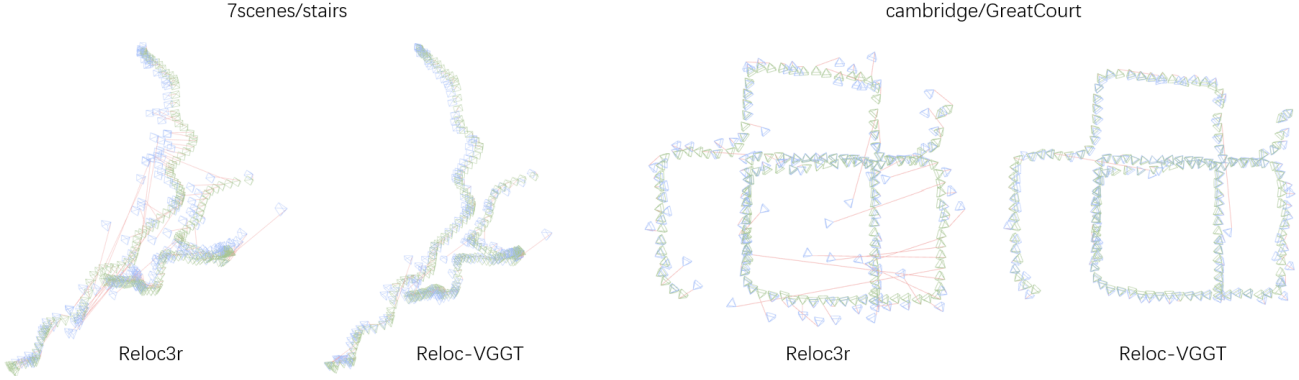


Figure 4. We visualize pose estimates for two scenes: stairs from the 7 Scenes dataset [62] and GreatCourt from Cambridge Landmarks [34]. We compare our results with the existing sota method Reloc3R [31].

Model Variant	7-Scenes (Avg.)	Cambridge Landmarks (Avg.)	Inference Time (s)
	Trans. (m) / Rot. (°)	Trans. (m) / Rot. (°)	
a. w/o RPTP & SMA (VGGT)	0.034/0.908	0.39/0.40	4.74
b. w/o RPTP	0.051/1.241	0.64/1.16	3.10
c. w/o SMA	0.031/0.896	0.37/0.38	4.82
d. w RPTP & SMA	0.039/1.033	0.48/0.55	3.14

Table 5. Ablation Study on Core Components of Reloc-VGGT. RPTP: Relative Pose Tokenizer and Projection. SMA: Sparse Mask Attention.

Mask type	chess	fire	heads	Inference time
Global Attention	0.025/0.767	0.024/0.833	0.013/0.770	4.82
Causal Attention	0.039/0.898	0.034/1.013	0.019/0.894	4.71
Masked Attention	0.027/0.861	0.028/0.871	0.014/0.818	3.14
Dilated Attention	0.026/0.837	0.027/0.864	0.013/0.809	4.03

Table 6. Pose estimation accuracy (translation error (m) / rotation error (°)) and inference time per sequence(s) under different masking strategies on the 7-Scenes dataset.

model achieves an optimal balance between accuracy and efficiency. In Tab. 6, we evaluate the impact of different mask types on final performance. We observe that, although the sparse mask attention incurs a slight accuracy drop compared with the dilated mask, it offers significantly better real-time performance. In contrast, the causal mask performs poorly in both accuracy and speed. These results demonstrate that our sparse mask design is well aligned with the characteristics of the visual localization task, as it prioritizes attention around the query pose token where information is most critical.

We further analyzed the impact of  $K$  (the number of retrieved database frames) on performance, where  $K$  ranges from 10 to 80, covering typical settings in visual relocalization tasks. The experimental results are shown in Fig. 5. It is evident that when  $K$  increases, the visual localization accuracy improves. This is attributed to the richer spatial context provided by more source frames. However, when  $K$  exceeds 20, accuracy gains saturate while inference time increases substantially. The original global attention mech-

anism in VGGT exhibits a quadratic growth with respect to the number of frames, while our method achieves linear-time scaling. This substantially improves the practicality of our framework and greatly enhances its deployment potential in real-world scenarios.

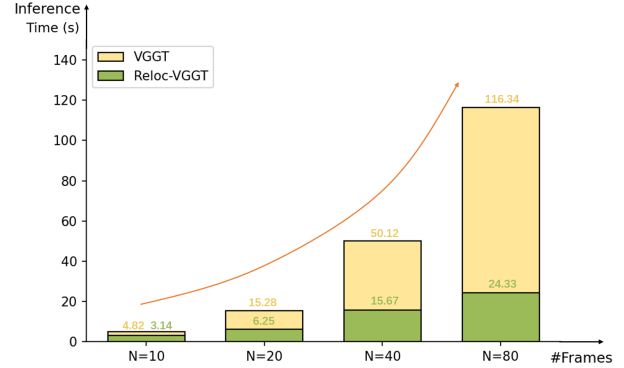


Figure 5. We visualize the runtime trend as the number of selected top- $k$  images increases, comparing the global attention mechanism with our proposed sparse mask attention. Our sparse mask attention strategy significantly reduces inference time, making relocalization over longer sequences computationally feasible.

## 4.6. Conclusion

In this paper, we propose Reloc-VGGT, a novel visual relocalization framework with 3D foundation model. We introduce a pose tokenizer and projection module that ef-

fectively inject the spatial information from source frames into the attention blocks. Furthermore, we design a sparse mask attention mechanism that reduces the computational complexity from quadratic to linear, significantly enhancing real-time performance and scalability. Extensive experiments demonstrate that our method achieves superior performance in terms of generalization ability and pose estimation accuracy, highlighting the effectiveness of multi-view spatial integration for visual relocalization.

## References

[1] Relja Arandjelovic, Petr Gronat, Akihiko Torii, Tomas Pajdla, and Josef Sivic. Netvlad: Cnn architecture for weakly supervised place recognition. In *Proceedings of the IEEE conference on computer vision and pattern recognition*, pages 5297–5307, 2016. 3, 4, 5

[2] Eduardo Arnold, Jamie Wynn, Sara Vicente, Guillermo Garcia-Hernando, Aron Monszpart, Victor Prisacariu, Daniyar Turmukhambetov, and Eric Brachmann. Map-free visual relocalization: Metric pose relative to a single image. In *European Conference on Computer Vision*, pages 690–708. Springer, 2022. 2, 6, 7

[3] Jinze Bai, Shuai Bai, Yunfei Chu, Zeyu Cui, Kai Dang, Xiaodong Deng, Yang Fan, Wenbin Ge, Yu Han, Fei Huang, et al. Qwen technical report. *arXiv preprint arXiv:2309.16609*, 2023. 3

[4] Yutong Bai, Xinyang Geng, Karttikeya Mangalam, Amir Bar, Alan L Yuille, Trevor Darrell, Jitendra Malik, and Alexei A Efros. Sequential modeling enables scalable learning for large vision models. In *Proceedings of the IEEE/CVF Conference on Computer Vision and Pattern Recognition*, pages 22861–22872, 2024. 3

[5] Vassileios Balntas, Shuda Li, and Victor Prisacariu. Relocnet: Continuous metric learning relocalisation using neural nets. In *Proceedings of the European conference on computer vision (ECCV)*, pages 751–767, 2018. 2, 7

[6] Eric Brachmann and Carsten Rother. Learning less is more: 6d camera localization via 3d surface regression. In *Proceedings of the IEEE conference on computer vision and pattern recognition*, pages 4654–4662, 2018. 1

[7] Eric Brachmann and Carsten Rother. Visual camera relocalization from rgb and rgb-d images using dsac. *IEEE transactions on pattern analysis and machine intelligence*, 44(9):5847–5865, 2021. 7

[8] Eric Brachmann, Tommaso Cavallari, and Victor Adrian Prisacariu. Accelerated coordinate encoding: Learning to relocalize in minutes using rgb and poses. In *Proceedings of the IEEE/CVF Conference on Computer Vision and Pattern Recognition*, pages 5044–5053, 2023. 1

[9] Samarth Brahmbhatt, Jinwei Gu, Kihwan Kim, James Hays, and Jan Kautz. Geometry-aware learning of maps for camera localization. In *Proceedings of the IEEE conference on computer vision and pattern recognition*, pages 2616–2625, 2018. 1

[10] Yohann Cabon, Lucas Stoffl, Leonid Antsfeld, Gabriela Csurka, Boris Chidlovskii, Jerome Revaud, and Vincent Leroy. Must3r: Multi-view network for stereo 3d reconstruction. In *Proceedings of the Computer Vision and Pattern Recognition Conference*, pages 1050–1060, 2025. 3, 6

[11] Le Chen, Weirong Chen, Rui Wang, and Marc Pollefeys. Leveraging neural radiance fields for uncertainty-aware visual localization. In *2024 IEEE International Conference on Robotics and Automation (ICRA)*, pages 6298–6305. IEEE, 2024. 2

[12] Shuai Chen, Xinghui Li, Zirui Wang, and Victor A Prisacariu. Dfnet: Enhance absolute pose regression with direct feature matching. In *European Conference on Computer Vision*, pages 1–17. Springer, 2022. 7

[13] Shuai Chen, Yash Bhalgat, Xinghui Li, Jia-Wang Bian, Kejie Li, Zirui Wang, and Victor Adrian Prisacariu. Neural refinement for absolute pose regression with feature synthesis. In *Proceedings of the IEEE/CVF Conference on Computer Vision and Pattern Recognition*, pages 20987–20996, 2024. 7

[14] Shuai Chen, Tommaso Cavallari, Victor Adrian Prisacariu, and Eric Brachmann. Map-relative pose regression for visual re-localization. In *Proceedings of the IEEE/CVF Conference on Computer Vision and Pattern Recognition*, pages 20665–20674, 2024. 7

[15] Aakanksha Chowdhery, Sharan Narang, Jacob Devlin, Maarten Bosma, Gaurav Mishra, Adam Roberts, Paul Barham, Hyung Won Chung, Charles Sutton, Sebastian Gehrmann, et al. Palm: Scaling language modeling with pathways. *Journal of Machine Learning Research*, 24(240):1–113, 2023. 3

[16] Ronald Clark, Sen Wang, Andrew Markham, Niki Trigoni, and Hongkai Wen. Vidloc: A deep spatio-temporal model for 6-dof video-clip relocalization. In *Proceedings of the IEEE conference on computer vision and pattern recognition*, pages 6856–6864, 2017. 2

[17] Angela Dai, Angel X. Chang, Manolis Savva, Maciej Halber, Thomas Funkhouser, and Matthias Niessner. Scannet: Richly-annotated 3d reconstructions of indoor scenes. In *Proceedings of the IEEE Conference on Computer Vision and Pattern Recognition (CVPR)*, 2017. 5, 6

[18] Tri Dao. Flashattention-2: Faster attention with better parallelism and work partitioning. *arXiv preprint arXiv:2307.08691*, 2023. 5

[19] Tianchen Deng, Siyang Liu, Xuan Wang, Yeqia Liu, Danwei Wang, and Weidong Chen. Prosgnerf: Progressive dynamic neural scene graph with frequency modulated auto-encoder in urban scenes. *arXiv preprint arXiv:2312.09076*, 2023. 2

[20] Tianchen Deng, Yaohui Chen, Leyan Zhang, Jianfei Yang, Shenghai Yuan, Danwei Wang, and Weidong Chen. Compact 3d gaussian splatting for dense visual slam. *arXiv preprint arXiv:2403.11247*, 2024. 1

[21] Tianchen Deng, Guole Shen, Tong Qin, Jianyu Wang, Wentao Zhao, Jingchuan Wang, Danwei Wang, and Weidong Chen. Plgslam: Progressive neural scene representation with local to global bundle adjustment. In *Proceedings of the IEEE/CVF Conference on Computer Vision and Pattern Recognition*, pages 19657–19666, 2024. 1

[22] Tianchen Deng, Xun Chen, Ziming Li, Hongming Shen, Danwei Wang, Javier Civera, and Hesheng Wang. Unipr3d: Towards universal visual place recognition with visual

geometry grounded transformer. *arXiv preprint 2512.21078*, 2025. 4

[23] Tianchen Deng, Yue Pan, Shanghai Yuan, Dong Li, Chen Wang, Mingrui Li, Long Chen, Lihua Xie, Danwei Wang, Jingchuan Wang, Javier Civera, Hesheng Wang, and Weidong Chen. What is the best 3d scene representation for robotics? from geometric to foundation models. *arXiv preprint arXiv:2512.03422*, 2025. 3

[24] Tianchen Deng, Guole Shen, Xun Chen, Shanghai Yuan, Hongming Shen, Guohao Peng, Zhenyu Wu, Jingchuan Wang, Lihua Xie, Danwei Wang, Hesheng Wang, and Weidong Chen. Mcn-slam: Multi-agent collaborative neural slam with hybrid implicit neural scene representation. *arXiv preprint arXiv:2506.18678*, 2025. 2

[25] Tianchen Deng, Guole Shen, Chen Xun, Shanghai Yuan, Tongxin Jin, Hongming Shen, Yanbo Wang, Jingchuan Wang, Hesheng Wang, Danwei Wang, et al. Mne-slam: Multi-agent neural slam for mobile robots. In *Proceedings of the Computer Vision and Pattern Recognition Conference*, pages 1485–1494, 2025. 1

[26] Tianchen Deng, Nailin Wang, Chongdi Wang, Shanghai Yuan, Jingchuan Wang, Hesheng Wang, Danwei Wang, and Weidong Chen. Incremental joint learning of depth, pose and implicit scene representation on monocular camera in large-scale scenes. *IEEE Transactions on Automation Science and Engineering*, pages 1–1, 2025. 2

[27] Tianchen Deng, Yanbo Wang, Hongle Xie, Hesheng Wang, Rui Guo, Jingchuan Wang, Danwei Wang, and Weidong Chen. Neslam: Neural implicit mapping and self-supervised feature tracking with depth completion and denoising. *IEEE Transactions on Automation Science and Engineering*, pages 1–1, 2025. 2

[28] Tianchen Deng, Wenhua Wu, Junjie He, Yue Pan, Xirui Jiang, Shanghai Yuan, Danwei Wang, Hesheng Wang, and Weidong Chen. Vpgs-slam: Voxel-based progressive 3d gaussian slam in large-scale scenes. *arXiv preprint arXiv:2505.18992*, 2025. 1

[29] Daniel DeTone, Tomasz Malisiewicz, and Andrew Rabinovich. Superpoint: Self-supervised interest point detection and description. In *Proceedings of the IEEE Conference on Computer Vision and Pattern Recognition (CVPR) Workshops*, 2018. 1, 2

[30] Mingyu Ding, Zhe Wang, Jiankai Sun, Jianping Shi, and Ping Luo. Camnet: Coarse-to-fine retrieval for camera relocalization. In *Proceedings of the IEEE/CVF International Conference on Computer Vision*, pages 2871–2880, 2019. 2, 7

[31] Siyan Dong, Shuzhe Wang, Shaohui Liu, Lulu Cai, Qingnan Fan, Juho Kannala, and Yanchao Yang. Reloc3r: Large-scale training of relative camera pose regression for generalizable, fast, and accurate visual localization. In *Proceedings of the Computer Vision and Pattern Recognition Conference*, pages 16739–16752, 2025. 2, 3, 5, 6, 7, 8

[32] Johan Edstedt, Qiyu Sun, Georg Bökman, Mårten Wadenbäck, and Michael Felsberg. Roma: Robust dense feature matching. In *Proceedings of the IEEE/CVF Conference on Computer Vision and Pattern Recognition*, pages 19790–19800, 2024. 6

[33] Alex Kendall and Roberto Cipolla. Geometric loss functions for camera pose regression with deep learning. In *Proceedings of the IEEE conference on computer vision and pattern recognition*, pages 5974–5983, 2017. 1

[34] Alex Kendall, Matthew Grimes, and Roberto Cipolla. Posenet: A convolutional network for real-time 6-dof camera relocalization. In *Proceedings of the IEEE international conference on computer vision*, pages 2938–2946, 2015. 5, 7, 8

[35] Alex Kendall, Matthew Grimes, and Roberto Cipolla. Posenet: A convolutional network for real-time 6-dof camera relocalization. In *Proceedings of the IEEE international conference on computer vision*, pages 2938–2946, 2015. 2

[36] Bernhard Kerbl, Georgios Kopanas, Thomas Leimkühler, and George Drettakis. 3d gaussian splatting for real-time radiance field rendering. *ACM Trans. Graph.*, 42(4):139–1, 2023. 1, 2

[37] Alexander Kirillov, Eric Mintun, Nikhila Ravi, Hanzi Mao, Chloe Rolland, Laura Gustafson, Tete Xiao, Spencer Whitehead, Alexander C Berg, Wan-Yen Lo, et al. Segment anything. In *Proceedings of the IEEE/CVF international conference on computer vision*, pages 4015–4026, 2023. 3

[38] Zakaria Laskar, Iaroslav Melekhov, Surya Kalia, and Juho Kannala. Camera relocalization by computing pairwise relative poses using convolutional neural network. In *Proceedings of the IEEE international conference on computer vision workshops*, pages 929–938, 2017. 7

[39] Vincent Leroy, Yohann Cabon, and Jérôme Revaud. Grounding image matching in 3d with mast3r. In *European Conference on Computer Vision*, pages 71–91. Springer, 2024. 6

[40] Xiaotian Li, Shuzhe Wang, Yi Zhao, Jakob Verbeek, and Juho Kannala. Hierarchical scene coordinate classification and regression for visual localization. In *Proceedings of the IEEE/CVF Conference on Computer Vision and Pattern Recognition*, pages 11983–11992, 2020. 1

[41] Amy Lin, Jason Y Zhang, Deva Ramanan, and Shubham Tulsiani. Relpose++: Recovering 6d poses from sparse-view observations. In *2024 International Conference on 3D Vision (3DV)*, pages 106–115. IEEE, 2024. 6

[42] Jingyu Lin, Jiaqi Gu, Bojian Wu, Lubin Fan, Renjie Chen, Ligang Liu, and Jieping Ye. Learning neural volumetric pose features for camera localization. In *European Conference on Computer Vision*, pages 198–214. Springer, 2024. 7

[43] Philipp Lindenberger, Paul-Edouard Sarlin, Viktor Larsson, and Marc Pollefeys. Pixel-perfect structure-from-motion with featuremetric refinement. In *Proceedings of the IEEE/CVF international conference on computer vision*, pages 5987–5997, 2021. 6

[44] Shuhong Liu, Tianchen Deng, Heng Zhou, Liuzhuozheng Li, Hongyu Wang, Danwei Wang, and Mingrui Li. Mg-slam: Structure gaussian splatting slam with manhattan world hypothesis. *IEEE Transactions on Automation Science and Engineering*, 2025. 2

[45] Will Maddern, Geoffrey Pascoe, Chris Linegar, and Paul Newman. 1 year, 1000 km: The oxford robotcar dataset. *The International Journal of Robotics Research*, 36(1):3–15, 2017. 6

[46] Ben Mildenhall, Pratul P. Srinivasan, Matthew Tancik, Jonathan T. Barron, Ravi Ramamoorthi, and Ren Ng. Nerf: Representing scenes as neural radiance fields for view synthesis. In *ECCV*, 2020. 1, 2, 4

[47] Shervin Minaee, Tomas Mikolov, Narjes Nikzad, Meysam Chenaghlu, Richard Socher, Xavier Amatriain, and Jianfeng Gao. Large language models: A survey. *arXiv preprint arXiv:2402.06196*, 2024. 3

[48] Arthur Moreau, Nathan Piasco, Dzmitry Tsishkou, Bogdan Stanciulescu, and Arnaud de La Fortelle. Lens: Localization enhanced by nerf synthesis. In *Conference on Robot Learning*, pages 1347–1356. PMLR, 2022. 2, 7

[49] Raúl Mur-Artal, J. M. M. Montiel, and Juan D. Tardós. Orb-slam: A versatile and accurate monocular slam system. *IEEE Transactions on Robotics*, 31(5):1147–1163, 2015. 1, 2

[50] Maxime Oquab, Timothée Darcet, Théo Moutakanni, Huy Vo, Marc Szafraniec, Vasil Khalidov, Pierre Fernandez, Daniel Haziza, Francisco Massa, Alaaeldin El-Nouby, et al. Dinov2: Learning robust visual features without supervision. *arXiv preprint arXiv:2304.07193*, 2023. 4

[51] William Peebles and Saining Xie. Scalable diffusion models with transformers. In *Proceedings of the IEEE/CVF international conference on computer vision*, pages 4195–4205, 2023. 3

[52] Tong Qin, Peiliang Li, and Shaojie Shen. Vins-mono: A robust and versatile monocular visual-inertial state estimator. *IEEE Transactions on Robotics*, 34(4):1004–1020, 2018. 1, 2

[53] Jeremy Reizenstein, Roman Shapovalov, Philipp Henzler, Luca Sbordone, Patrick Labatut, and David Novotny. Common objects in 3d: Large-scale learning and evaluation of real-life 3d category reconstruction. In *Proceedings of the IEEE/CVF international conference on computer vision*, pages 10901–10911, 2021. 5, 6

[54] Soham Saha, Girish Varma, and CV Jawahar. Improved visual relocalization by discovering anchor points. *arXiv preprint arXiv:1811.04370*, 2018. 7

[55] Paul-Edouard Sarlin, Daniel DeTone, Tomasz Malisiewicz, and Andrew Rabinovich. Superglue: Learning feature matching with graph neural networks. In *Proceedings of the IEEE/CVF conference on computer vision and pattern recognition*, pages 4938–4947, 2020. 1, 2

[56] Johannes L Schonberger and Jan-Michael Frahm. Structure-from-motion revisited. In *Proceedings of the IEEE conference on computer vision and pattern recognition*, pages 4104–4113, 2016. 4

[57] Yoli Shavit, Ron Ferens, and Yosi Keller. Learning multi-scene absolute pose regression with transformers. In *Proceedings of the IEEE/CVF International Conference on Computer Vision*, pages 2733–2742, 2021. 1

[58] Yoli Shavit, Ron Ferens, and Yosi Keller. Coarse-to-fine multi-scene pose regression with transformers. *IEEE transactions on pattern analysis and machine intelligence*, 45(12):14222–14233, 2023. 1

[59] Guole Shen, Tianchen Deng, Yanbo Wang, Yongtao Chen, Yilin Shen, Jiuming Liu, and Jingchuan Wang. Grs-slam3r: Real-time dense slam with gated recurrent state. *arXiv preprint arXiv:2509.23737*, 2025. 2

[60] Hongming Shen, Xun Chen, Yulin Hui, Zhenyu Wu, Wei Wang, Qiyang Lyu, Tianchen Deng, and Danwei Wang. Unilgl: Learning uniform place recognition for fov-limited/panoramic lidar global localization. *arXiv preprint arXiv:2507.12194*, 2025. 1

[61] You Shen, Zhipeng Zhang, Yansong Qu, and Liujuan Cao. Fastvggt: Training-free acceleration of visual geometry transformer. *arXiv preprint arXiv:2509.02560*, 2025. 4

[62] Jamie Shotton, Ben Glocker, Christopher Zach, Shahram Izadi, Antonio Criminisi, and Andrew Fitzgibbon. Scene coordinate regression forests for camera relocalization in rgb-d images. In *Proceedings of the IEEE conference on computer vision and pattern recognition*, pages 2930–2937, 2013. 5, 6, 7, 8

[63] Mehmet Ozgur Turkoglu, Eric Brachmann, Konrad Schindler, Gabriel J Brostow, and Aron Monszpart. Visual camera re-localization using graph neural networks and relative pose supervision. In *2021 International Conference on 3D Vision (3DV)*, pages 145–155. IEEE, 2021. 3

[64] Ashish Vaswani, Noam Shazeer, Niki Parmar, Jakob Uszkoreit, Llion Jones, Aidan N Gomez, Łukasz Kaiser, and Illia Polosukhin. Attention is all you need. *Advances in neural information processing systems*, 30, 2017. 3

[65] Florian Walch, Caner Hazirbas, Laura Leal-Taixe, Torsten Sattler, Sebastian Hilsenbeck, and Daniel Cremers. Image-based localization using lstms for structured feature correlation. In *Proceedings of the IEEE international conference on computer vision*, pages 627–637, 2017. 1

[66] Jianyuan Wang, Christian Rupprecht, and David Novotny. Posediffusion: Solving pose estimation via diffusion-aided bundle adjustment. In *Proceedings of the IEEE/CVF International Conference on Computer Vision*, pages 9773–9783, 2023. 5, 6

[67] Jianyuan Wang, Nikita Karaev, Christian Rupprecht, and David Novotny. Vggfsm: Visual geometry grounded deep structure from motion. In *Proceedings of the IEEE/CVF conference on computer vision and pattern recognition*, pages 21686–21697, 2024. 6

[68] Jianyuan Wang, Minghao Chen, Nikita Karaev, Andrea Vedaldi, Christian Rupprecht, and David Novotny. Vggt: Visual geometry grounded transformer. In *Proceedings of the Computer Vision and Pattern Recognition Conference*, pages 5294–5306, 2025. 2, 3, 4, 5

[69] Shuzhe Wang, Vincent Leroy, Yohann Cabon, Boris Chidlovskii, and Jerome Revaud. Dust3r: Geometric 3d vision made easy. In *Proceedings of the IEEE/CVF Conference on Computer Vision and Pattern Recognition*, pages 20697–20709, 2024. 2, 3, 5, 6

[70] Yifan Wang, Xingyi He, Sida Peng, Dongli Tan, and Xiaowei Zhou. Efficient loftr: Semi-dense local feature matching with sparse-like speed. In *Proceedings of the IEEE/CVF conference on computer vision and pattern recognition*, pages 21666–21675, 2024. 6

[71] Yanbo Wang, Zipeng Fang, Lei Zhao, and Weidong Chen. Learning to tune like an expert: Interpretable and scene-aware navigation via mllm reasoning and cvae-based adaptation. *arXiv preprint arXiv:2507.11001*, 2025. 2

[72] Zirui Wang, Shangzhe Wu, Weidi Xie, Min Chen, and Victor Adrian Prisacariu. Nerf-: Neural radiance fields without known camera parameters. *arXiv preprint arXiv:2102.07064*, 2021. [1](#)

[73] Dominik Winkelbauer, Maximilian Denninger, and Rudolph Triebel. Learning to localize in new environments from synthetic training data. In *2021 IEEE International Conference on Robotics and Automation (ICRA)*, pages 5840–5846. IEEE, 2021. [6](#), [7](#)

[74] Fei Xue, Xin Wang, Zike Yan, Qiuyuan Wang, Junqiu Wang, and Hongbin Zha. Local supports global: Deep camera relocalization with sequence enhancement. In *Proceedings of the IEEE/CVF International Conference on Computer Vision*, pages 2841–2850, 2019. [2](#)

[75] Botaq Ye, Sifei Liu, Haofei Xu, Xuetong Li, Marc Pollefeys, Ming-Hsuan Yang, and Songyou Peng. No pose, no problem: Surprisingly simple 3d gaussian splats from sparse unposed images. *arXiv preprint arXiv:2410.24207*, 2024. [6](#)

[76] Lin Yen-Chen, Pete Florence, Jonathan T. Barron, Alberto Rodriguez, Phillip Isola, and Tsung-Yi Lin. inerf: Inverting neural radiance fields for pose estimation. In *2021 IEEE/RSJ International Conference on Intelligent Robots and Systems (IROS)*, pages 1323–1330, 2021. [1](#), [2](#)

[77] Hongjia Zhai, Xiyu Zhang, Boming Zhao, Hai Li, Yijia He, Zhaopeng Cui, Hujun Bao, and Guofeng Zhang. Splatloc: 3d gaussian splatting-based visual localization for augmented reality. *IEEE Transactions on Visualization and Computer Graphics*, 2025. [2](#)

[78] Jason Y Zhang, Deva Ramanan, and Shubham Tulsiani. Relpose: Predicting probabilistic relative rotation for single objects in the wild. In *European Conference on Computer Vision*, pages 592–611. Springer, 2022. [6](#)

[79] Jason Y Zhang, Amy Lin, Moneish Kumar, Tzu-Hsuan Yang, Deva Ramanan, and Shubham Tulsiani. Cameras as rays: Pose estimation via ray diffusion. *arXiv preprint arXiv:2402.14817*, 2024. [6](#)

[80] Qunjie Zhou, Torsten Sattler, Marc Pollefeys, and Laura Leal-Taixe. To learn or not to learn: Visual localization from essential matrices. In *2020 IEEE International Conference on Robotics and Automation (ICRA)*, pages 3319–3326. IEEE, 2020. [2](#), [7](#)

[81] Dong Zhuo, Wenzhao Zheng, Jiahe Guo, Yuqi Wu, Jie Zhou, and Jiwen Lu. Streaming 4d visual geometry transformer. *arXiv preprint arXiv:2507.11539*, 2025. [4](#), [5](#)